Journal of the Earth and Space Physics, Vol. 41, No. 4, 2016, PP. 39-50

Development of a regional attenuation relationship for Alborz, Iran

Yazdani, A.[1*], Kowsari, M.[2] and Amani, S.[2]

1. Associate Professor, Department of Civil Engineering, University of Kurdistan, Sanandaj, Iran
2. Graduated Student, Department of Civil Engineering, University of Kurdistan, Sanandaj, Iran

(Received: 12 Aug 2014, Accepted: 31 Jan 2016)

Abstract

New attenuation relationships for rock and soil in Alborz, have been developed in this study. When the quantity of usable ground-motion data is inadequate in the magnitude and distance ranges, development of an empirical prediction equation is deficient. Due to lack of data, the two well-known simulation techniques, point source and finite-fault models have been used to generate more than ten thousands of strong motions as input data. The stochastic finite-fault modeling that can be used to predict regional groundmotion for large faults has been developed based on subdividing the fault surface into smaller subsources, as stochastic point sources. The model incorporates the seismological information obtained from recorded data of northern Iran to provide new information on source and path effects. In this study, the uncertainty due to inherent variability in earthquake source, path, and site effects has been considered. The results include the attenuation relationships that are validated by statistical analysis to compare the estimated ground motion with those of recorded data at the observed stations in Alborz region.

Keywords: Attenuation relationship, Alborz, Stochastic simulation, Uncertainty.

1. Introduction

An attenuation relationship, or ground motion prediction equation (GMPE) as seismologists prefer to call it, is a mathematical-based expression related to a specific strong-motion parameter such as peak ground acceleration (PGA) or response spectra. This is at a site with respect to the source-site distance *R*, earthquake magnitude *M*, and some other seismological parameters. It can quantitatively characterize the earthquake strength, source, the wave propagation path between the source and the site, and the soil and geological profile beneath the site (Nicknam et al., 2009). GMPEs have a major impact on seismic hazard estimates, because they control the predicted amplitudes of ground shaking (Ghofrani and Atkinson et al., 2014). In general, GMPEs are divided into empirical and physical based modeling. Empirical attenuation relationship was constructed to fit the available data for certain mathematical forms using different techniques in which the validity of these equations is basically dependent on sufficiency of the data. Development of mathematical models for prediction of ground motion is still a major challenge, particularly for the regions with scant observational data. The information contained in the available data set is not sufficient to properly constrain all of the regression coefficients for a given functional form (Arroyo and Ordaz, 2010). To handle this problem, theoretical models based on physical principles and seismological modeling would be a good choice to apply for incomplete recorded ground-motion data to develop an empirical model. The applicability of these models has been demonstrated for a particular area where detailed knowledge is available about the faults system, seismic source, and wave propagation characteristics (Ólafsson et al., 2001; Ólafsson and Sigbjörnsson, 1999, 2014).

Alborz is one of the highly seismic regions of Iran with an east–west-trending mountain belt. It is a folded and faulted area where extends for a distance of 960 km across the northern part of the country (Farrokhi et al., 2015). The active faults of the Alborz arises a continuous hazard to local population including the 12 million people in capital city of Tehran. They are situated along the southern margin of Alborz Mountain Range with the risk of future seismic events (Nazari et al., 2014). Moreover, the probability that large earthquakes exceed over 50 and 100 years is

[*]Corresponding author: E-mail: a.yazdani@uok.ac.ir

high in most parts of this region (Yazdani and Kowsari, 2013). Many destructive earthquakes have occurred in this region. As a result of the sparse distribution of strong-motion stations and the fact that most of the destructive earthquake events, especially in Alborz, date back to the time of the development of the Iranian strong motion network, there are insufficient ground-motion data to provide a complete database to develop empirical ground-motion prediction equations. To overcome such shortcoming and to properly reflect the inhomogeneity of the seismicity, thousands of strong motions were generated to incorporate a range value of source-path-site seismological/geological parameters. An attenuation relationship is developed for the region which reflects the attenuated peak ground acceleration and spectral acceleration of the generated strong motions from the source up to the site of interest, in different site condition. Among the currently used strong motion generation techniques, the two widely used stochastic point source/ finite fault models were used to estimate the strong motions.

2. Methodology

The modeling of strong motion at a particular site by seismological based approach includes three basic subjects. The first is to study source dynamics of ground-motion generation from faults. The second is seismic wave propagation effects due to complex geological structures in propagation-path from source to site including wave attenuation and scattering. The third is amplification and de-amplification of seismic motions due to surface geology and topography. The basic knowledge of source rupture and wave propagation from source-to-site based on elasto-dynamic theory is well established by Aki and Richards (2002). The two well-known simulation techniques, namely point-source and finite-fault methods, have been used by many investigators to synthesize destructive strong motions.

The point-source procedure originally presented by Brune (1970) and subsequently developed by Boore (1983, 2003), can identify the important factors in a few key parameters. The point source model is generic, simple to use, and appears most suitable for seismic hazard modeling of low seismicity areas where the details of the potential earthquake source are generally unknown. In spite of overall success, it is also well known that the point-source model breaks down in some cases, particularly near the source of large earthquakes. The effect of a large finite-fault, including rupture propagation, directivity, and source-receiver geometry, can profoundly influence the amplitudes, frequency content, and duration of ground-motion (Beresnev and Atkinson, 1997). A common approach to modeling of these effects is to subdivide the fault into smaller elements, each treated as a point source (Hartzell, 1978). In the typical implementation, the rupture is started at a hypocentral point on the fault and propagates radially from it, triggering the subfaults as it passes them. The fields from all sub-events are geometrically delayed and added together at the observation point (Beresnev and Atkinson, 2002).

The stochastic method is capable to combine parametric or functional descriptions of the ground motion amplitude spectrum with a random phase spectrum. This spectrum is modified and the motion is distributed over a duration related to the earthquake magnitude and to the distance from the source (Boore, 2003). The Fourier amplitude spectrum can be expressed as a product of a number of factors as:

$$A(f)=\frac{(2\pi)^2 R_{\theta\phi}F_s V}{4\pi\rho\beta^3}S(f)R^b\exp\left(\frac{-\pi fR}{\beta Q(f)}\right)P(f) \qquad (1)$$

where R is the closet distance to rupture area, $R_{\theta\varphi}$ is the average radiation pattern, F_S is the free-surface amplification, V partition of energy onto two horizontal components, ρ is density and β is shear-wave velocity in kilometers per second. The term $S(f) = M_0 f^2/(1+ (f/ f_c)^2)$ is Brune's (1970) source model, M_0 is seismic moment in dyne-cm and f_c is the corner frequency given by $f_c= 4.9\times10^6\beta(\Delta\sigma/M_0)^{1/3}$ where $\Delta\sigma$ is stress parameter in bars. The quality factor Q (f) as an inverse measure of anelastic attenuation determines the shape of the high frequency spectrum. The term $P(f) = exp(-\pi f\kappa)$ is a high-cut filter to model near-surface kappa effects; kappa is the commonly observed rapid spectral decay at high frequencies (Anderson and Hough, 1984). The term R^b is the geometric attenuation factor.

As mentioned before, in the finite fault

method, a large fault is divided into N subfaults and each subfault is considered as a small point. In the stochastic finite-fault modeling based on static corner frequency, the corner frequency of subfaults is defined as:

$$f_{cij} = 4.91\times10^{6}\beta\times(\frac{\Delta\sigma}{M_{0ij}})^{1/3} \quad (2)$$

In identical subfaults, the moment of each subfault is controlled by the ratio of its area to the area of the main fault ($M_{0ij}= M_0/N$, where M_0 is the seismic moment of the entire the fault). There are $nl\times nw$ sources on the fault plane, nl and nw are the number of subfaults along the length and width of main fault, respectively. If the subfaults are not identical the seismic moment of each subfault is expressed as (Motazedian and Atkinson, 2005):

$$M_{0ij} = \frac{M_0 S_{ij}}{\sum_{l=1}^{nl}\sum_{k=1}^{nw} S_{kl}} \quad (3)$$

where S_{ij} is the relative slip weight of the ij^{th} subfault. The ground motions of the subfaults are summed with a proper time delay in the time domain to obtain the ground motion acceleration, $a(t)$, from the entire fault (Hartzell, 1978):

$$a(t) = \sum_{i=1}^{nl}\sum_{j=1}^{nw} a_{ij}(t+\Delta t_{ij}) \quad (4)$$

where Δt_{ij} is the relative delay time for the radiated wave from the ij^{th} subfault to reach the observation point.

The main deficiency in use of the static corner frequency is that as the rupture propagates toward the end of the fault, the number of ruptured subfaults increases; hence, the corner frequency of the subfaults and of the radiated spectrum decreases (Boore, 2009). In stochastic finite-fault modeling based on dynamic corner frequency, a scaling factor is introduced to balance this tendency and conserve the total radiated energy of subfaults at high frequencies. The dynamic corner frequency of the subfaults are a function of time and is defined as a function of the cumulative number of ruptured subfaults, $N_R(t)$, at time t (Motazedian and Atkinson, 2005):

$$f_{cij\,dyn} = 4.91\times10^{6}\beta\times N_R^{-1/3}\times N^{1/3}(\frac{\Delta\sigma}{M_0})^{1/3} \quad (5)$$

In the time the rupture-propagation front finally reaches the end of the fault, the number of ruptured subfaults is $N_R(t)^{-1/3} = N^{1/3}$. Thus, the corner frequency at the end of rupture gives f_c, as the corner frequency of the entire fault. The scaling factor, H_{ij} is applied to conserve energy in the subfault summation, through a summation formulation based on normalization of the velocity spectrum (Atkinson et al., 2009):

$$H_{ij} = \left(N\sum\left\{ f/[1+(\frac{f}{f_c})^2]\right\}^2 / \sum\left\{ f/[1+(\frac{f}{f_{cij_{dyn}}})^2]\right\}^2 \right)^{0.5} \quad (6)$$

3. Data analysis

The functional form of attenuation relationship based on earthquake seismology can approximately be linearized by a simple expression of the following form:

$$\ln A(f) = c_1(f) + c_2(f)M + c_3(f)\ln R + c_4(f)R + \varepsilon \quad (7)$$

where ln represents natural logarithm, $A(f)$ is the strong-motion parameter; PGA and spectral acceleration in this study is represented in different periods for 5% of damping. In this relationship, M is the earthquake magnitude and R is the closest distance to the rupture area. The uncertainties are represented by the standard deviation of the residuals, σ_ε. The coefficients of c_1-c_4 are the regression coefficients. The functional form is developed for generic rock and generic soil consistent with site classification I/II and III/IV in Iranian Seismic Code (BHRC, 2005), respectively.

To develop the regional attenuation relationship, two different point-source and finite-fault methodologies have been used to simulate ground motions. The point-source model is reasonable when the source-to-site distance is much larger than the source dimensions (Atkinson and Silva, 1997; Boore, 2009). One widely used point-source simulation program, SMSIM (Boore, 2003), is used in simulation of far-distance earthquakes. The main advantage of this procedure is the speed of the calculations. There are important factors that influence ground motions. Some of the factors are not included in the stochastic point-source model, such as the effects of faulting geometry, heterogeneity of slip on the fault plane, and directivity. The computer code EXSIM-Beta (Motazedian and Atkinson,

2005) was used for generation of ground. The model based on dynamic corner frequency has several advantages over previous stochastic finite-fault models (FINSIM), including independence of the results from subfault size, conservation of radiated energy, and the ability to have only a portion of the fault active at any time during the rupture (Atkinson and Boore, 2006). The simulations for near and intermediate distances are performed with the EXSIM-Beta by the model of Mavroeidis and Papageorgiou (2003) for the near-fault effects and the proposed modifications (Atkinson et al., 2009; Boore, 2009). More than ten thousands ground motions were simulated using the EXSIM_Beta and SMSIM methodologies in the magnitude-distance ranges of interest (M 5 to7.5 at R 5 to 200 km) with the median parameters, including uncertainties.

Uncertainty is a capacious issue that arises from incomplete information, disagreement among information sources, linguistic imprecision, variability, quantity, and structure of a model (Morgan and Henrion, 1990). The uncertainty in basic variables is categorized as aleatory or epistemic. In this study, the uncertainty due to inherent variability in earthquake source, path, and site effects has an aleatory nature that cannot be reduced by acquiring additional data or information. Model uncertainty in the prediction relation may arise from missing certain variables in the mathematic model, perhaps due to our lack of knowledge about these missing variables or our desire to exclude them from the model for the sake of simplicity (Wang and Takada, 2009). Uncertainty in parameters, often called statistical uncertainty, is epistemic in nature. This uncertainty is directly related to the quantity and quality of the available observed data. In this study, we include aleatory uncertainty by treating each key parameter as a probability distribution, with the given median value and the random variability about that median. Uniform or truncated normal distributions are used to express the uncertainty, depending on the parameter being modeled. To properly consider epistemic uncertainty, one needs to consider a wide variety of alternative models and theories of ground motion (Atkinson and Boore, 2006). Thus, in this study we do not attempt to completely model the effects of this kind of uncertainty.

The algorithm for the one-stage maximum-likelihood method was used to derive the equations (Joyner and Boore, 1993). Equations were derived for the estimation of PGA and spectral acceleration for a 5% critical damping ratio and for 14 different periods between 0.1 s and 4.0 sec. The regression coefficients c_1 through c_4 for generic soil and rock sites at different periods are listed in Table 1.

Table 1. Regression coefficients based on generated data

	Soil					Rock				
Period (s)	C_1	C_2	C_3	C_4	σ	C_1	C_2	C_3	C_4	σ
PGA	3.713	0.666	-0.795	-0.004	0.6	4.095	0.588	-0.862	-0.002	0.6
0.1	4.547	0.645	-0.741	-0.004	0.6	4.857	0.581	-0.781	-0.004	0.6
0.2	3.806	0.714	-0.679	-0.006	0.6	3.973	0.661	-0.728	-0.004	0.6
0.3	3.012	0.790	-0.628	-0.008	0.6	3.009	0.749	-0.667	-0.006	0.6
0.4	2.241	0.867	-0.587	-0.009	0.6	2.157	0.833	-0.630	-0.007	0.6
0.5	1.529	0.939	-0.564	-0.010	0.6	1.371	0.911	-0.602	-0.008	0.6
0.6	0.926	1.000	-0.549	-0.011	0.6	0.738	0.973	-0.588	-0.009	0.6
0.7	0.145	1.083	-0.524	-0.011	0.6	-0.098	1.062	-0.566	-0.009	0.6
0.8	-0.454	1.146	-0.507	-0.012	0.6	-0.722	1.127	-0.546	-0.010	0.6
0.9	-1.092	1.216	-0.496	-0.012	0.6	-1.363	1.195	-0.531	-0.010	0.6
1	-1.410	1.245	-0.492	-0.013	0.6	-1.813	1.242	-0.520	-0.011	0.6
1.5	-3.700	1.495	-0.452	-0.015	0.6	-3.972	1.473	-0.486	-0.013	0.6
2	-5.215	1.646	-0.438	-0.017	0.6	-5.551	1.637	-0.474	-0.014	0.6
3	-7.086	1.831	-0.427	-0.019	0.6	-7.473	1.828	-0.461	-0.016	0.6
4	-8.070	1.912	-0.434	-0.020	0.6	-8.523	1.919	-0.454	-0.019	0.6

4. Results and Discussions

Stochastic point-source and finite-fault methodologies are used to develop regional ground-motion prediction equations. To enable reliable seismic hazard estimation, the prediction of the source, path, and site parameters in a seismological model is important. In generation of ground-motions, the average radiation pattern is $R_{\theta\varphi}$=0.55, the free-surface amplification is F_S=2, and the partition of energy onto two horizontal components is V=0.707. Density and shear wave velocity are also selected as 2.8 g/cm^3 and 3.5 km/s, respectively. The empirical relationship proposed by Wells and Coppersmith (1994) is used to obtain the fault dimensions and the moment magnitude.

The stress parameter controlling the amplitude of high frequency radiation is one of the most important parameters in the simulation. For Northern Iran, Motazedian (2006) suggested average stress parameters of 125 bars and 68 bars for point-source and finite-fault methodologies, respectively. As mentioned before in considering aleatory uncertainty in input parameters, the stress parameter is modeled as a normal distribution. In this case, the logarithm of the stress is normally distributed with mean 2.1 bars and standard deviation 0.3. The percentage of the fault pulsing at any time has an influence on the relative amount of low frequency radiation. Several studies indicated the similarity between attenuation characteristics of Iran and California (Chandra et al., 1979; Nuttli, 1980; Chen and Atkinson, 2002; Shoja-Taheri et al., 2005). For this reason and because of the fact that we do not have any information about percentage-pulsing area in Northern Iran, this parameter is assumed based on calibration studies with California data, a uniform distribution from 10% to 90% which is shown as a relatively large aleatory variability (Atkinson and Boore, 2006).

The geometric attenuation, the attenuation of spectral amplitudes with distance is described by a trilinear relationship. The *b*-value, geometric spreading coefficient, should be determined at different distances for any possible multi-segment behavior due to post-critical reflection effect from Moho (Burger et al., 1987) and domination of multiply reflected and refracted shear waves at larger distances (Herrmann and Kijko, 1983). Based on 139 vertical component records of the Kojour earthquake, it is indicated that the best fit to data is given by $R^{-1.0}$, $R^{+0.2}$, and $R^{-0.1}$ for distances up to 70 km, from 70 to 150 km, and more than 150 km, respectively (Motazedian, 2006).

The Quality factor is determined by regression on the shear-wave Fourier amplitude spectra. It indicated the wave-transmission quality of rock and depends on seismotectonic features of the region. In Northern Iran, Motazedian (2006) indicated that this factor has a U–shaped behavior as $\log(Q) = 1.99(\log f^2) - 0.67(\log f) + 2.32$. The effects of the near-surface attenuation are taken into account by diminishing the simulated spectra by the kappa factor. The mean value of kappa for horizontal components in Alborz is assumed equal to 0.05 (Motazedian, 2006; Mousavi et al., 2007; Soghrat et al., 2012). The aleatory uncertainty in this parameter is represented by a uniform distribution from 0.03 to 0.06.

JICA (2000) using the data from the distribution of micro-earthquake activities recommended the dip angle of the faults in northern Iran about 75 degree. In this study, it is assumed that the dip angle has a normal distribution with mean value and standard deviation equal to 75 and 25, respectively. Previous studies indicated that reliable earthquake depths in the Alborz are less than 15 km (Jackson et al., 2002; Maggi et al., 2003). A mean focal depth of 12 km and standard deviation of 8 km by normal distribution is considered for all of the faults. We chose the recommended amplification factor by Boore and Joyner (1997) for generic rock (V_{s30}= 620 m/s) and generic soil (V_{s30}= 310 m/s) consistent with site classification I/II and III/IV in Iranian Code (BHRC, 2005), respectively. Recently, Soghrat et al. (2012) obtained the site effects for Northern Iran. The effects were completely consistent with the model proposed by Boore and Joyner (1997).

Figure 1 shows the decay of estimated peak ground acceleration and spectral acceleration at 1 s natural period with distance for Mw =5, 6 and 7 at a rock site. As expected, this figure reveals that the amplitude of ground motion is decreased with increasing distance. Figure 2 shows a

comparison between the local site amplification factors for soil and rock sites derived in this study. This figure shows the estimated response spectra for Mw = 5, 6 and 7 at 10 and at 100km in two different site classes. As it is expected, the amplitudes in soil have a higher content at higher periods.

In Attenuation relationships, the standard deviation of strong ground motion parameter is used to show the uncertainty of estimated values. As discussed before, the standard deviation of ground motion parameter is presented as aleatory uncertainty. The aleatory uncertainty is independent of magnitude and distance, with an average value of 0.60 natural logarithm units for all periods which is consistent with the value of uncertainty in previous studies for Iranian attenuation relationships.

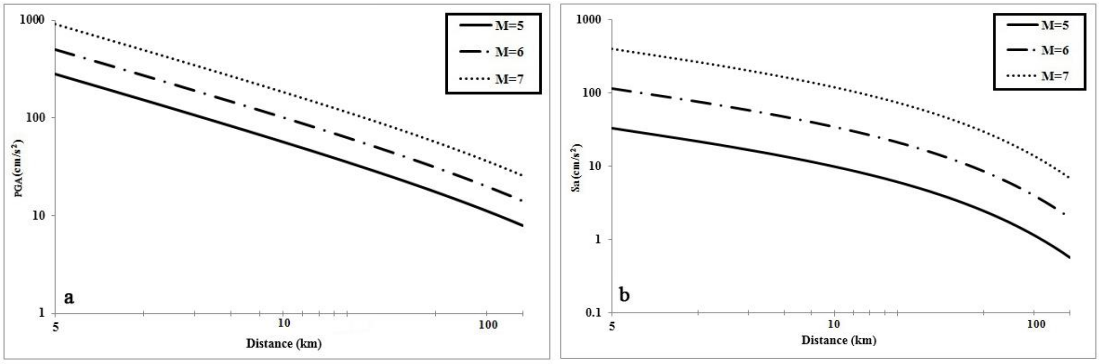

(a) **(b)**

Fig. 1. (a) Decay of estimated peak ground acceleration and (b) spectral acceleration at 1 s natural period with distance for Mw =5, 6 and 7 at a rock site

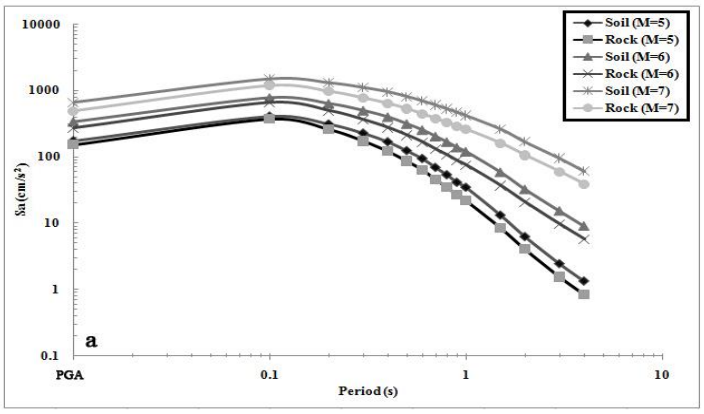

(a)

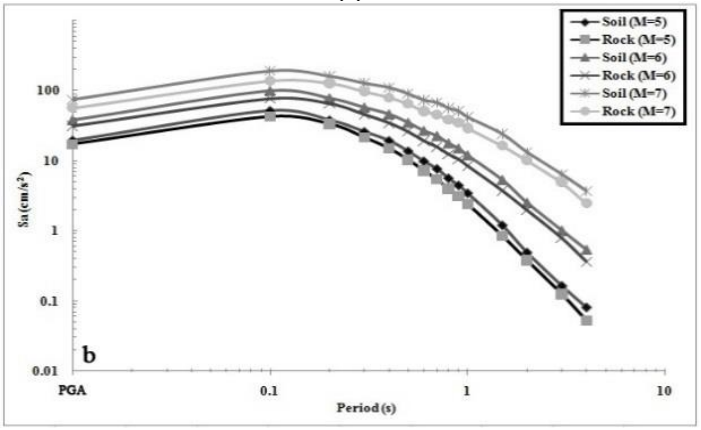

(b)

Fig. 2. Spectral acceleration for magnitude Mw=5, 6 and 7 at two different site conditions at, (a)10 km, (b)100 km

Figure 3 compares the median of estimated ground motions for an event of M_w=6 at different distances in two different site classes from the equations derived in this study with those of Ambraseys et al. (2005), Nowroozi (2005), Ghasemi et al. (2009), Ghodrati et al. (2007, 2010), and Saffari et al. (2012). In comparison, the used ground motion parameters are PGA and spectral accelerations at 0.2 and 1.0 sec because of the importance of these periods in the earthquake engineering. The prediction equation of Ambraseys et al. (2005) is applicable to Europe and the Middle East for shallow crustal earthquakes, and other prediction equations are based on records of Iranian earthquakes and therefore are very suitable for comparison. In the study of Ghodrati et al. (2007, 2010), the magnitude scale is based on surface wave magnitude (M_S), so the presented relationship by Nowroozi (2005) is used to convert surface magnitude to moment magnitude. All of the other equations were derived by the same magnitude scale, and consequently, no conversions had to be applied.

The predicted PGA and spectral amplitudes from the equations presented here are not much different from those predicted by other recent ground-motion estimation equations in Iran. This result shows that estimates of the ground motions for such earthquakes are well defined, and the estimates are stable. Previous equations have usually been derived using sets of records with a lack of data from the near-field and large events; therefore, these equations have not been well-constrained for such magnitudes and distances. For assessment of the validity of the presented model, the attenuation is compared with the recorded data in Alborz. The database with magnitudes greater than 5 and PGA>0.05g and known soil type (Sinaeian, 2006) are gathered from the Iranian Strong-Motion Network of the Building and Housing Research Center (BHRC 2014). Also, in order to avoid the uncertainty, empirical conversion formulated from other magnitude scales to M_w were not used and the only magnitude used here is the moment magnitude based on the Harvard Centroid Moment Tensor database (HRVD-CMT 2014). The used recorded data in comparison are shown in Table A1. Figure 4 shows the residuals between the recorded and predicted values against M_w and distance for PGA and spectral acceleration at 0.2 and 1.0 second. This figure indicates good match of the model with the recorded data.

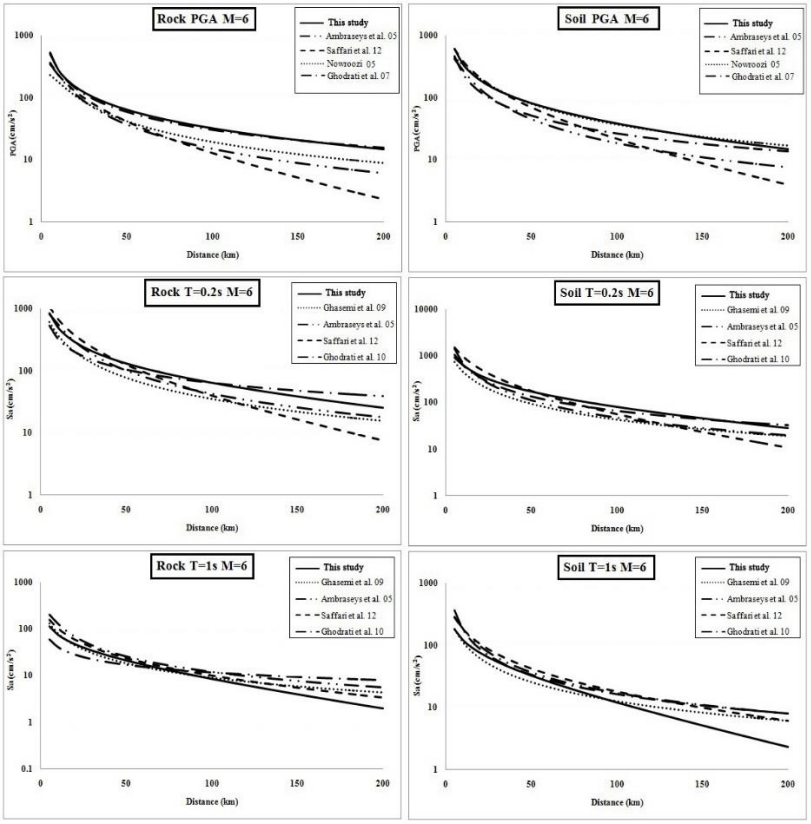

Fig. 3. Comparison of proposed relationship with other studies

Finally, we used two robust statistical techniques, the likelihood (LH) (Scherbaum et al., 2004) and Log-likelihood (LLH) (Scherbaum et al., 2009) methods, to assess the compatibility between the observed and predicted data. The results for the PGA and the selected periods T=0.2 and T=1s have been shown in Table 2. The goodness-of-fit measures are the LLH value, median of LH value, the median, mean, and standard deviation of the normalized residuals, which herein are abbreviated as LLH, MEDLH, MEDNR, MEANNR, and STDNR, respectively. Also, the corresponding standard deviations of these measures (σ), have been estimated by the bootstrap technique. The results of LH and LLH analysis show that the presented model is dramatically in good agreement with the observed ground motions.

Table 2. The results of LH and LLH methods for interested periods

PGA									
Model	**LLH**	**MEDLH**	**σ**	**MEDNR**	**σ**	**MEANNR**	**σ**	**STDNR**	**σ**
This study	**1.212**	**0.512**	**0.057**	**0.654**	**0.082**	**0.706**	**0.068**	**0.607**	**0.071**
N05	**1.727**	**0.519**	**0.079**	**0.643**	**0.120**	**0.755**	**0.067**	**0.602**	**0.057**
A05	**2.112**	**0.266**	**0.060**	**1.110**	**0.131**	**1.180**	**0.091**	**0.819**	**0.067**
S12	**1.918**	**0.346**	**0.072**	**0.941**	**0.145**	**1.137**	**0.099**	**0.899**	**0.077**
G07	**2.067**	**0.231**	**0.046**	**1.195**	**0.114**	**1.286**	**0.100**	**0.876**	**0.080**
T=0.2s									
Model	**LLH**	**MEDLH**	**σ**	**MEDNR**	**σ**	**MEANNR**	**σ**	**STDNR**	**σ**
This study	**1.351**	**0.433**	**0.061**	**0.783**	**0.099**	**0.832**	**0.068**	**0.607**	**0.050**
G09	**2.245**	**0.246**	**0.052**	**1.158**	**0.117**	**1.171**	**0.081**	**0.733**	**0.045**
A05	**1.820**	**0.453**	**0.065**	**0.748**	**0.120**	**0.989**	**0.077**	**0.695**	**0.044**
S12	**1.756**	**0.313**	**0.055**	**1.008**	**0.116**	**1.091**	**0.086**	**0.779**	**0.055**
G10	**1.675**	**0.470**	**0.053**	**0.721**	**0.082**	**0.820**	**0.067**	**0.603**	**0.051**
T=1s									
Model	**LLH**	**MEDLH**	**σ**	**MEDNR**	**σ**	**MEANNR**	**σ**	**STDNR**	**σ**
This study	**1.601**	**0.480**	**0.056**	**0.705**	**0.104**	**0.944**	**0.077**	**0.720**	**0.064**
G09	**1.723**	**0.483**	**0.048**	**0.700**	**0.078**	**0.836**	**0.067**	**0.615**	**0.041**
A05	**1.539**	**0.487**	**0.056**	**0.693**	**0.085**	**0.793**	**0.065**	**0.619**	**0.049**
S12	**1.511**	**0.410**	**0.084**	**0.822**	**0.145**	**0.914**	**0.069**	**0.669**	**0.049**
G10	**1.598**	**0.568**	**0.047**	**0.570**	**0.072**	**0.697**	**0.057**	**0.540**	**0.042**

Note: Nowroozi, 2005 (N05); Ambraseys et al., 2005 (A05); Saffari et al., 2012 (S12); Ghodrati et al., 2007 (G07); Ghasemi et al., 2009 (G09); Ghodrati et al., 2010 (G10)

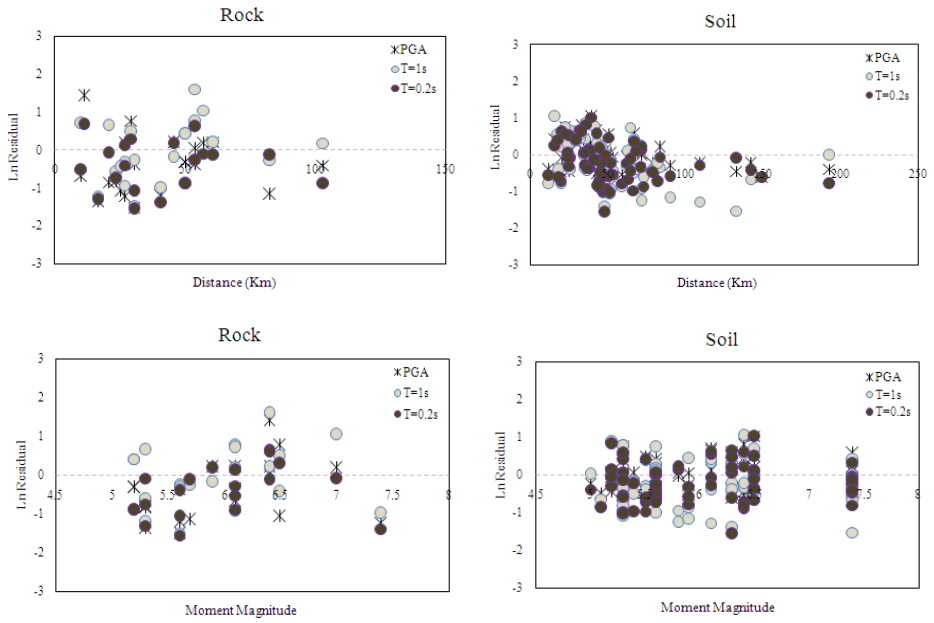

Fig. 4. Residuals between the observed and predicted model at different distances for PGA and spectral acceleration at 0.2 and 1.0 s

5. Conclusions

The new ground-motion relationships provide a good description of peak ground motions and response spectra for Alborz earthquakes. Since the detailed characteristics of future earthquakes are not known, the majority of earthquake design spectra are obtained by weighted averaging of a set of response spectra from the records with similar characteristics such as soil condition, epicentral distance, magnitude and source mechanism (Javan-emrooz et al., 2014). When the quantity of usable ground-motion data is inadequate in the magnitude and distance ranges, the development of an empirical prediction equation is deficient. In this case, it is possible to use simple seismological models that can be initially used to describe how ground motion scales with earthquake source size and source-to-site distance. Due to lack of data, the two widely used stochastic techniques and point source/finite fault models were used to generate the ground-motion as input data to develop the attenuation relationship of this site.

To generate data, most key parameters are taken from Motazedian (2006) because the EXSIM_BETA program had been calibrated for Alborz in Motazedian (2006). In the present study, thousands of ground motions have been generated with the vast variability for each parameter. They certainly cover all possible results that might be obtained by the other studies such as Zafarani et al. (2008), Hamzehloo et al. (2010) and Soghrat et al. (2012) which indeed had compatible results with Motazedian (2006).

In developing attenuation relation, the uncertainties inherently existing in the seismological/geotechnical parameters were reduced by generating thousands of the data incorporating a range of these values in the model. The underlying model parameters, such as the source spectrum and attenuation, are modified by the recorded data for moderate events. The model predictions are compared with northern Iran ground-motion data and with predictions of other equations to test the predictive power of the ground-motion relationships developed in this study. There are insufficient strong-motion data to adequately judge the relationships at large magnitudes, although they appear to be consistent with the available earthquake data in Alborz, especially in high frequencies.

Acknowledgments

We thank the Building and Housing Research Centre of Iran for providing the database. The authors would like to thank the anonymous reviewers whose valuable suggestions lead to significant improvements in the manuscript.

References

Aki, K. and Richards, P. G., 2002, Quantitative seismology: theory and methods, University Science Books, Sausalito, CA.

Ambraseys, N. N., Douglas, J., Sarma, S. K. and Smit, P. M., 2005, Equations for the estimation of strong ground motions from shallow crustal earthquakes using data from Europe and the Middle East: horizontal peak ground acceleration and spectral acceleration, Bulletin of Earthquake Engineering, 3, 1-53.

Anderson, J. and Hough, S., 1984, A model for the shape of the Fourier amplitude spectrum of acceleration at high frequencies, Bulletin of the Seismological Society of America, 74, 1969-1993.

Arroyo, D. and Ordaz, M., 2010, Multivariate Bayesian regression analysis applied to ground-motion prediction equations, part 1: theory and synthetic example, Bulletin of the Seismological Society of America, 100, 1551-1567.

Atkinson, G. and Boore D. M., 2006, Earthquake ground-motion prediction equations for Eastern North America, Bulletin of the Seismological Society of America, 96, 2181-2205.

Atkinson, G. and Silva, W., 1997, An empirical study of earthquake source spectra for California earthquakes, Bulletin of the Seismological Society of America, 87, 97-113.

Atkinson, G., Boore, D. M., Assatourians, K., Campbell, K. W. and Motazedian, D., 2009, A guide to differences between stochastic point source and stochastic finite fault simulations, Bulletin of the Seismological Society of America, 99, 3192-3201.

Beresnev, I. and Atkinson, G., 1997, Modeling finite fault radiation from the ω_n spectrum, Bulletin of the Seismological Society of America, 87, 67-84.

Beresnev, I. and Atkinson, G., 2002, Source parameters of earthquakes in eastern and western North America based on finite-fault modeling, Bulletin of the Seismological Society of America, 92, 695-710.

Boore, D. M. and Joyner, W., 1997, Site amplifications for generic rock sites, Bulletin of the Seismological Society of America, 87, 327-341.

Boore, D. M., 1983, Stochastic simulation of high-frequency ground motions based on seismological models of the radiated spectra, Bulletin of the Seismological Society of America, 73, 1865-1894.

Boore, D. M., 2003, Prediction of ground motion using the stochastic method, Pure and Applied Geophysics, 160, 635-676.

Boore, D. M., 2009, Comparing stochastic point- and finite-source ground-motion simulations: SMSIM and EXSIM, Bulletin of the Seismological Society of America, 99, 3202-3216.

Brune, J. N., 1970, Tectonic stress and the spectra of seismic shear waves from earthquakes, Journal of Geophysical Research, 75, 4997-5009.

Building and Housing Research Center, 2005, Iranian Code of Practice for Seismic Resistant Design of Buildings Standard No. 2800, Third Revision, Iran (In Persian).

Building and Housing Research Center, 2014, http://www.bhrc.ac.ir. Last accessed 08Jan 2014

Burger, R., Somerville, P., Barker, J., Herrmann, R. and Helmberger, D., 1987, The effect of crustal structure on strong ground motion attenuation relations in eastern North America, Bulletin of the Seismological Society of America, 77, 420-439.

Chandra, V. J., McWhorten, G. and Nowroozi, A., 1979, Attenuation of intensities in Iran, Bulletin of the Seismological Society of America, 69, 237-250.

Chen, S. Z. and Atkinson, G. M., 2002, Global comparisons of earthquake source spectra, Bulletin of the Seismological Society of America, 92, 885-895.

Farrokhi, M., Hamzehloo, H., Rahimi, H. and Allamehzadeh, M., 2015, Estimation of coda-wave attenuation in the Central and Eastern Alborz, Iran, Bulletin of the Seismological Society of America, 105, 1756-1767.

Ghasemi, H., Zare, M., Fukushima, Y. and Koketsu, K., 2009, An empirical spectral ground-motion model for Iran, Journal of Seismology, 13, 499-515.

GhodratiAmiri, G., Khorasani, M., MirzaHessabi, R. and RazavianAmrei, S. A., 2010, Ground-motion prediction equations of spectral ordinates and arias intensity for Iran, Journal of Earthquake Engineering, 14, 1-29.

GhodratiAmiri, G., Mahdavian, A. and Manouchehri Dana, F., 2007, Attenuation relationships for Iran, Journal of Earthquake Engineering, 11, 469-92.

Ghofrani, H. and Atkinson, G., 2014, Ground-motion prediction equations for interface earthquakesof M7 to M9 based on empirical data from Japan, Bulletin of the Earthquake Engineering, 12, 549-571.

Hamzehloo, H., Rahimi, H., Sarkar, I., Mahood, M., MirzaeiAlavijeh, H. and Farzanegan, E., 2010, Modeling the strong ground motion and rupture characteristics of the March 31, 2006, Darb-e-Astane earthquake, Iran, using a hybrid of near-field SH-wave and empirical Green's function method, Journal of seismology 14, 169-195.

Hartzell, S., 1978, Earthquake aftershocks as Green's functions, Geophysical Research Letters, 5, 1-14.

Harvard Seismology, 2014, Centroid moment tensor (CMT) catalog search, www.seismology.harvard.edu/.

Herrmann, R. and Kijko, A., 1983, Modeling some empirical vertical component Lg relations, Bulletin of the Seismological Society of America, 73, 157-171.

Jackson, J., Priestley, K., Allen, M. and Berberian, M., 2002, Active tectonics of the South Caspian Basin, Geophysical Journal International, 148, 214-245.

Japan International Cooperation Agency (JICA), 2000, The study on seismic microzoning of the greater Tehran area in the Islamic Republic of Iran, Final report to the Government of the Islamic Republic of Iran, Tokyo, Japan.

Javan-emrooz, H. R., EskandariGhadi, M. and Mirzaei, N., 2014, Magnitude and distance dependent design spectra for rock sites based on Iranian acceleration time-histories and comparison with regional design spectra, Journal of the Earth and Space Physics, 40, 1-16 (In Persian).

Joyner, W. B. and Boore, D. M., 1993, Methods for regression analysis of strong-motion data, Bulletin of the Seismological Society of America, 83, 469-487.

Maggi, A., Priestly, K. and Jackson, J., 2003, Focal depths of moderate and large size earthquakes in Iran, Journal of Seismology

and Earthquake Engineering, 4, 1-10.

Mavroeidis, G. and Papageorgiou, A., 2003, A mathematical representation of near-fault ground motions, Bulletin of the Seismological Society of America, 93, 1099-1131.

Morgan, M. G. and Henrion, M., 1990, Uncertainty: a guide to dealing with uncertainty in quantitative risk and policy analysis. Cambridge University Press, New York.

Motazedian, D. and Atkinson, G., 2005, Stochastic finite-fault modeling based on a dynamic corner frequency, Bulletin of the Seismological Society of America, 95, 995-1010.

Motazedian, D., 2006, Region-specific key seismic parameters for earthquakes in Northern Iran, Bulletin of the Seismological Society of America, 96, 1383-1395.

Mousavi, M., Zafarani, H., Noorzad, A., Ansari, A. and Bargi, K., 2007, Analysis of Iranian strong-motion data using the specific barrier model, Journal of Geophysical Engineering, 4, 1-14.

Nazari, H., Ritz, H. F., Walker, R. T., Salamati, R., Rizza, M., Patnaik R., Hollingsworth, J., Alimohammadian, H., Jalali, A., KavehFirouz, A. and Shahidi, A., 2014, Palaeoseismic evidence for a medieval earthquake and preliminary estimate of late Pleistocene slip-rate, on the Firouzkuh strike-slip fault in the Central Alborz region of Iran, Journal of Asian Earth Sciences, 82, 124-135.

Nicknam, A., Yazdani, A. and YaghmaeiSabegh, S., 2009, Predicting probabilistic-based Strong ground motion time series for citadel of Arg-E-Bam (south-east of Iran), Journal of Earthquake Engineering, 13, 482-499.

Nowroozi, A., 2005, Attenuation relations for peak horizontal and vertical accelerations of earthquake ground motion in Iran: a preliminary analysis, Journal of Seismology and Earthquake Engineering, 7, 109-128.

Nuttli, O. W., 1980, The excitation, and attenuation of seismic crustal phases in Iran, Bulletin of the Seismological Society of America, 70, 469-485.

Ólafsson, S. and Sigbjörnsson, R., 1999, A theoretical attenuation model for earthquake-induced ground motion, Journal of earthquake engineering, 3, 287-315.

Ólafsson, S. and Sigbjörnsson, R., 2014, Ground motion prediction equation for south Iceland, second European conference on earthquake engineering and semiology, Istanbul.

Ólafsson, S., Remseth, S. and Sigbjörnsson, R., 2001, Stochastic models for simulation of strong ground motion in Iceland, Earthquake Engineering and Structural Dynamics, 30, 1305-1331.

Saffari, H., Kuwata, Y., Takada, S. and Mahdavian, A., 2012, Updated PGA, PGV, and spectral acceleration attenuation relations for Iran, Earthquake Spectra, 28, 1-20.

Scherbaum, F., Cotton, F. and Smit, P., 2004, On the use of response spectral reference data for the selection of ground-motion models for seismic hazard analysis: the case of rock motion, Bulletin of the Seismological Society of America, 94, 2164-2185.

Scherbaum, F., Delavaud, E. and Riggelsen, C., 2009, Model selection in seismic hazard analysis: an information-theoretic perspective, Bulletin of the Seismological Society of America, 99, 3234-3247.

Shoja-Taheri, J., Naserieh, S. and Ghafoorian-Nasab, A. H., 2005, The 2003 Bam, Iran, earthquake: an interpretation of the strong motion records, Earthquake Spectra, 21, S181-206.

Sinaeian, F., 2006, Study on Iran strong motion records, PhD dissertation, International Institute of Earthquake Engineering and Seismology, Tehran, Iran.

Soghrat, M. R., Khaji, N. and Zafarani, H., 2012, Simulation of strong ground motion in northern Iran using the specific barrier model, Geophys. J. Int., 188, 645-679.

Wang, M. and Takada, T., 2009, A Bayesian framework for prediction of seismic ground motion, Bulletin of the Seismological Society of America, 99, 2348-2364.

Wells, D. L. and Coppersmith, K. J., 1994, New empirical relationships among magnitude, rupture length, rupture width, rupture area and surface displacement, Bulletin of the Seismological Society of America, 84, 974-1002.

Yazdani, A. and Kowsari, M., 2013, Bayesian estimation of seismic hazards in Iran, ScientiaIranica, 20, 422-430.

Zafarani, H., Mousavi, M., Noorzad, A. and Ansari A., 2008, Calibration of the specific barrier model to Iranian plateau earthquakes

and development of physically based attenuation relationships for Iran, Soil Dynamic and Earthquake Engineering, 28, 550-576.

Appendix

Table A1. Characteristics of the Alborz records

Station	Record ID	Date Y-M-D	Time H:M:S	M_w	Lat. (EQ)	Lon. (EQ)	Lat. (Station)	Lon. (Station)	Soil Type
Maku	1046-1	1976-11-24	12:22:25	7.0	39.12	43.92	39.30	44.51	R
Talesh	1098-2	1978-11-04	15:22:22	6.3	37.67	48.90	37.80	48.90	S
Lahijan	1150	1980-07-22	05:17:06	5.5	37.36	50.35	37.21	50.03	S
Rudsar	1151	1980-07-22	05:17:06	5.5	37.36	50.35	37.13	50.30	S
Rudsar	1185	1980-12-03	04:26:15	5.3	37.17	50.47	37.13	50.30	S
Oroomiyeh4	1188	1981-07-23	00:05:30	5.8	37.11	45.21	37.55	45.07	S
Oroomiyeh3	1189	1981-07-23	00:05:30	5.8	37.10	45.21	37.55	45.07	S
Polsefid	1373	1990-01-20	01:27:10	5.9	35.89	53.00	36.11	53.05	S
Qazvin	1353-1	1990-06-20	21:00:11	7.4	36.96	49.41	36.26	50.00	S
Abhar	1354	1990-06-20	21:00:11	7.4	36.99	49.35	36.09	49.22	S
Rudsar	1355	1990-06-20	21:00:11	7.4	36.99	49.35	37.13	50.30	S
Lahijan	1357-1	1990-06-20	21:00:11	7.4	36.99	49.35	37.21	50.03	S
Tonkabon	1359	1990-06-20	21:00:11	7.4	36.96	49.41	36.80	50.88	S
Gachsar	1361	1990-06-20	21:00:11	7.4	36.96	49.41	36.11	51.32	S
Abbar	1362-1	1990-06-20	21:00:11	7.4	36.96	49.41	36.92	48.95	R
Zanjan	1364	1990-06-20	21:00:11	7.4	36.96	49.41	36.66	48.50	S
Eshtehard	1372	1990-06-20	21:00:11	7.4	36.96	49.41	35.72	50.37	S
Abbar	1362-8	1990-06-21	09:02:15	5.7	36.63	49.79	36.92	48.95	R
Manjil	1360	1990-06-24	09:46:01	5.3	36.88	49.42	36.76	49.39	R
Manjil	1377-1	1990-07-06	19:34:54	5.3	36.91	49.30	36.76	49.39	R
Sef. Dam4	1418	1991-11-28	17:19:58	5.6	36.92	49.60	36.75	49.39	R
Sef. Dam3	1419-1	1991-11-28	17:19:58	5.6	36.92	49.60	36.75	49.39	R
Rudbar2	1420-4	1991-11-28	17:19:58	5.6	36.92	49.60	36.80	49.40	R
Ardabil1	1693-1	1997-02-28	12:57:45	6.1	38.07	48.06	38.22	48.27	R
Ardabil2	1701-1	1997-02-28	12:57:45	6.1	38.22	48.26	38.07	48.06	S
Garmi	1702	1997-02-28	12:57:45	6.1	39.05	48.05	38.07	48.06	S
Hoorand	1716	1997-02-28	12:57:45	6.1	38.89	47.37	38.07	48.06	R
Namin	1724	1997-02-28	12:57:45	6.1	38.42	48.47	38.07	48.06	R
Sarab	1725	1997-02-28	12:57:45	6.1	37.93	47.54	38.07	48.06	S
Hal Abad	1733	1997-02-28	12:57:45	6.1	37.92	48.42	38.07	48.06	S
Kariq	1833-2	1997-02-28	12:57:45	6.1	37.92	48.06	38.07	48.06	R
Kariq	1833-15	1997-03-02	18:29:42	5.3	37.92	48.06	37.86	47.87	R
Garmi	2008-1	1998-07-09	14:19:18	5.9	39.05	48.06	38.72	48.51	S
Razi	2033-1	1998-07-09	14:19:18	5.9	38.63	48.09	38.72	48.51	R
Ziveh	2041	1998-07-09	14:19:18	5.9	39.11	47.65	38.72	48.51	S
Gomeyshan	2299	1999-11-19	04:40:24	5.4	37.07	54.07	37.34	54.40	S
Torkaman	2345	1999-11-19	04:40:24	5.4	36.89	54.06	37.34	54.40	S
Pars Abad	2411-1	2000-03-21	14:07:47	5.1	39.65	47.91	39.95	48.23	S
ChehelZarei	2465-1	2000-05-03	09:01:18	5.0	29.49	50.85	29.66	50.80	S
Jirandeh	2705-2	2002-04-19	13:46:49	5.2	36.70	49.79	36.56	49.88	S
Bakandi	2787-1	2002-04-19	13:46:49	5.2	36.4	49.57	36.56	49.88	S
Ziyaz	2976-1	2002-04-19	13:46:49	5.2	36.88	50.23	36.56	49.88	R
Abegarm	2748-1	2002-06-22	02:58:20	6.5	35.75	49.28	35.71	49.02	S
Avaj	2749-1	2002-06-22	02:58:20	6.5	35.58	49.22	35.71	49.02	R
Kab. Ahang	2754-1	2002-06-22	02:58:20	6.5	35.20	48.72	35.71	49.02	S
Razan	2756-1	2002-06-22	02:58:20	6.5	35.39	49.03	35.71	49.02	S
Abhar	2763	2002-06-22	02:58:20	6.5	36.15	49.22	35.71	49.02	S
Darsjin	2769-2	2002-06-22	02:58:20	6.5	36.02	49.23	35.71	49.02	R
Ghahvard	2778	2002-06-22	02:58:20	6.5	35.46	48.05	35.71	49.02	S
Shirinsoo	2781	2002-06-22	02:58:20	6.5	35.48	48.45	35.71	49.02	S
Pool	3330-1	2004-05-28	12:38:46	6.3	36.30	51.56	36.40	51.58	S
Hasankeif	3333	2004-05-28	12:38:46	6.3	36.30	51.56	36.50	51.15	S
Nowshahr	3368-1	2004-05-28	12:38:46	6.3	36.30	51.56	36.65	51.49	S
Noor	3369-1	2004-05-28	12:38:46	6.3	36.30	51.56	36.57	52.01	S
Roodsar	3373	2004-05-28	12:38:46	6.3	36.30	51.56	37.14	50.28	S
Aliabad	3542	2004-10-07	21:46:18	5.6	36.90	54.84	37.11	54.52	S
Gorgan	3545	2004-10-07	21:46:18	5.6	36.84	54.38	37.11	54.52	S
Gomeyshan	3546	2004-10-07	21:46:18	5.6	37.07	54.07	37.11	54.52	S
Ramiyan	3551	2004-10-07	21:46:18	5.6	37.02	55.14	37.11	54.52	S
AghGhala	3556-1	2004-10-07	21:46:18	5.6	37.01	54.46	37.11	54.52	S
BandareGaz	3557-2	2004-10-07	21:46:18	5.6	36.76	53.95	37.11	54.52	S
Inche Boron	3560-1	2004-10-07	21:46:18	5.6	37.45	54.72	37.11	54.52	S
Kowsar Dam	3561-1	2004-10-07	21:46:18	5.6	36.81	54.54	37.11	54.52	S
Vashm. Dam	3562-1	2004-10-07	21:46:18	5.6	37.21	54.74	37.11	54.52	S
Minoodasht	3654-1	2004-10-07	21:46:18	5.6	37.23	55.36	37.11	54.52	S
Gomeyshan	3607	2005-01-10	18:47:30	5.3	37.07	54.07	37.12	54.54	S
AghGhala	3608	2005-01-10	18:47:30	5.3	37.01	54.46	37.12	54.54	S
Inche Boron	3618	2005-01-10	18:47:30	5.3	37.45	54.72	37.12	54.54	S
Miane	3879	2005-09-26	18:57:12	5.2	37.43	47.70	37.34	47.82	S
Soltan Abad	3881	2005-09-26	18:57:04	5.2	37.34	47.82	37.08	47.93	S
Varzaghan	5579-1	2012-08-11	12:23:20	6.4	38.52	46.86	38.51	46.64	S
Khajeh	5547-1	2012-08-11	12:23:20	6.4	38.52	46.86	38.15	46.59	S
Ahar	5520-1	2012-08-11	12:23:20	6.4	38.52	46.86	38.47	47.06	S
Nahand	5558-1	2012-08-11	12:23:20	6.4	38.52	46.86	38.25	46.47	S
Haris	5540-1	2012-08-11	12:23:20	6.4	38.52	46.86	38.25	47.12	S
Mesh. Shahr	5602-1	2012-08-11	12:23:20	6.4	38.52	46.86	38.39	47.67	R
Kalaybar	5545-1	2012-08-11	12:23:20	6.4	38.52	46.86	38.87	47.04	R
Damirchi	5532-1	2012-08-11	12:23:20	6.4	38.52	46.86	38.12	47.37	R
Varzaghan	5589-7	2012-08-14	14:02:25	5.5	38.38	46.76	38.51	46.64	S
Khajeh	5608-4	2012-08-14	14:02:25	5.5	38.38	46.76	38.15	46.59	S
Varzaghan	5589-8	2012-08-15	17:49:04	5.3	38.35	46.61	38.51	46.64	S
Khajeh	5608-5	2012-08-15	17:49:04	5.3	38.35	46.61	38.15	46.59	S
Ahar	5591-5	2012-08-15	17:49:04	5.3	38.35	46.61	38.47	47.06	S
Varzaghan	5674-5	2012-11-07	06:26:31	5.3	38.45	46.52	38.51	46.64	